THE JOURNAL OF BIOLOGICAL CHEMISTRY
Vol. 273, No. 14, Issue of April 3, pp. 7835–7842, 1998
Printed in U.S.A.

DNA Structural Elements Required for ERCC1-XPF Endonuclease Activity*

(Received for publication, October 1, 1997, and in revised form, November 23, 1997)

Wouter L. de Laat, Esther Appeldoorn, Nicolaas G. J. Jaspers, and Jan H. J. Hoeijmakers‡

From the Department of Cell Biology and Genetics, Medical Genetics Centre, Erasmus University, P. O. Box 1738, 3000 DR Rotterdam, The Netherlands

The heterodimeric complex ERCC1-XPF is a structure-specific endonuclease responsible for the 5′ incision during mammalian nucleotide excision repair (NER). Additionally, ERCC1-XPF is thought to function in the repair of interstrand DNA cross-links and, by analogy to the homologous Rad1-Rad10 complex in *Saccharomyces cerevisiae*, in recombination between direct repeated DNA sequences. To gain insight into the role of ERCC1-XPF in such recombinational processes and in the NER reaction, we studied in detail the DNA structural elements required for ERCC1-XPF endonucleolytic activity. Recombinant ERCC1-XPF, purified from insect cells, was found to cleave stem-loop substrates at the DNA junction in the absence of other proteins like replication protein A, showing that the structure-specific endonuclease activity is intrinsic to the complex. Cleavage depended on the presence of divalent cations and was optimal in low Mn^{2+} concentrations (0.2 mM). A minimum of 4–8 unpaired nucleotides was required for incisions by ERCC1-XPF. Splayed arm and flap substrates were also cut by ERCC1-XPF, resulting in the removal of 3′ protruding single-stranded arms. All incisions occurred in one strand of duplex DNA at the 5′ side of a junction with single-stranded DNA. The exact cleavage position varied from 2 to 8 nucleotides away from the junction. One single-stranded arm, protruding either in the 3′ or 5′ direction, was necessary and sufficient for correct positioning of incisions by ERCC1-XPF. Our data specify the engagement of ERCC1-XPF in NER and allow a more direct search for its specific role in recombination.

Nucleotide excision repair (NER)[1] guards the integrity of the genome by removing bulky adducts and the most prominent UV-induced lesions from the DNA. During NER, the damaged DNA strand is incised asymmetrically around the lesion to allow release of the damage as part of a 24–32-nucleotide DNA fragment, followed by resynthesis and ligation (1–3). Whereas the latter steps are accomplished by general replication factors such as proliferating cell nuclear antigen, replication factor C, DNA polymerase δ, and/or ϵ and ligase, the incision stage of NER requires the action of XP factors (XPA-G) (4). XPA, and perhaps XPC complexed with hHR23B, are thought to be involved in damage recognition; XPB and XPD, two helicases present in the basal transcription factor complex TFIIH, and replication protein A (RPA) presumably demarcate the lesion by local opening of the DNA; XPG and the heterodimeric complex ERCC1-XPF perform the actual DNA cleavage. The role of XPE is, as yet, unclear. Mutations in either of the XP factors can cause the extreme UV-sensitive and cancer-prone phenotype observed with *Xeroderma pigmentosum* (XP) patients. Some human XP genes cross-complement the NER defect of laboratory induced UV-sensitive Chinese hamster mutant cell lines, subdivided into 10 complementation groups. Human XPF, for example, corrects the repair-defect of rodent group 4 cell lines. The human excision repair cross-complementing gene ERCC1 corrects rodent group 1 cell lines, but no ERCC1-deficient patients are known. ERCC1 and XPF form an endonuclease that incises the damaged strand 15–24 nucleotides away at the 5′ side of the lesion (5, 6). Cleavage by ERCC1-XPF and XPG, which makes the 3′ incision during NER, presumably occurs in a structure-specific manner, as both NER nucleases cut artificial DNA substrates preferentially at duplex single-stranded junctions (6, 7). Incisions made by ERCC1-XPF and XPG during NER co-localize to the borders of the opened DNA intermediate (8) and protein-protein interactions with other NER factors are likely to determine the exact positioning of both nucleases. For ERCC1-XPF, interactions with XPA and RPA have been reported (9–12).

The counterpart of ERCC1-XPF in *Saccharomyces cerevisiae*, Rad10-Rad1, is required not only for NER but also for recombination between direct repeated DNA sequences, a process which is also called single strand annealing (13, 14). By analogy, ERCC1-XPF is expected to fulfil a similar role in mammalian cells, and the two homologous protein complexes have been proposed to remove 3′ protruding single-stranded arms from recombined duplex regions (13, 15). Chinese hamster mutant cell lines defective in either ERCC1 (group 1) or XPF (group 4) are unique among the other NER-deficient mutants in that they show an extreme sensitivity to DNA cross-linking agents such as cisplatin and mitomycin C (16). Repair of interstrand cross-links probably also requires a recombinational event.

To gain insight in the role of ERCC1-XPF in such recombinational processes and in the NER reaction, it is of importance to define its DNA substrate specificity. Similar studies with the FEN-1 family of structure-specific nucleases revealed interesting characteristics of individual members. Flap endonuclease-1 (FEN-1), implicated in both *in vitro* replication (17) and *in vitro* repair (18), was found to cleave branched DNA structures with 5′ protruding single-stranded arms (flaps, splayed arms), but not with closed single-stranded regions (loops, bubbles) (19). XPG, also a member of this family and as yet only known to be involved in NER, cleaves both stem-loop and bubble substrates

* This work was supported by the Dutch Scientific Organization (NWO, Foundation for Chemical Research) and the Louis Jeantet Award. The costs of publication of this article were defrayed in part by the payment of page charges. This article must therefore be hereby marked "*advertisement*" in accordance with 18 U.S.C. Section 1734 solely to indicate this fact.

‡ To whom correspondence should be addressed. E-mail: hoeijmakers@gen.fgg.eur.nl; Tel.: 31-10-4087199; Fax: 31-10-4360225.

[1] The abbreviations used are: NER, nucleotide excision repair; XP, *Xeroderma pigmentosum*; RPA, replication protein A; ERCC, excision repair cross-complementing; FEN, flap endonuclease; MEF, mouse embryonal fibroblast; nt, nucleotide(s); PAGE, polyacrylamide gel electrophoresis; HA, peptide derived from influenza virus hemagglutinin.

as well as flaps and splayed arms (7, 8). Similar results were obtained with the *S. cerevisiae* homolog of XPG, Rad2, and all three members of this nuclease family cleaved DNA with similar polarity, *i.e.* in one strand of duplex DNA at the 3′ side of the junction with single-stranded DNA (20, 21). The differences in substrate specificity between XPG and Rad2 on the one hand and FEN-1 on the other, may point at their different roles in the cell. The well defined structural DNA requirements of FEN-1 have been the key to the recent disclosure of its role *in vitro* in a base excision repair subpathway (18). ERCC1-XPF, and its yeast homolog Rad1-Rad10, are not part of a larger family of structure-specific nucleases. Rad1-Rad10 was previously shown to cleave flaps, splayed arms, stem-loops, and bubbles at the 5′ side of duplex single-stranded junctions (22). Intriguingly, the sole domain shared between ERCC1 and FEN-1 nucleases, a presumed helix-hairpin-helix motif present twice at the C terminus of ERCC1, is lacking in Rad10 (23, 24). This double motif, in total approximately 50 residues long, is assumed to be involved in non-sequence specific DNA binding (25) and might endow ERCC1-XPF with additional properties or altered substrate specificity compared with Rad1-Rad10.

Here we report a detailed analysis of the DNA structural elements required for ERCC1-XPF cleavage. We found that ERCC1-XPF needs at least 4–8 unpaired nucleotides to cleave stem-loop substrates. Single-stranded arms protruding in the 3′ direction were efficiently removed by ERCC1-XPF from splayed arm and flap substrates. Incisions occurred in duplex DNA at the 5′ side of a junction with single-stranded DNA. Both 3′ and 5′ protruding arms could be used by ERCC1-XPF for correctly positioning its nuclease activity. These data provide a framework to envisage ERCC1-XPF activity in repair as well as in recombinational pathways.

EXPERIMENTAL PROCEDURES

Construction of Recombinant Baculoviruses—The construction of a cDNA encoding ERCC1 with a C-terminal 6xHis-tag was described previously (6). The 3′ end (*Nco*I-*Bam*HI) of this cDNA was used to replace the 3′ end (*Nco*I-*Bam*HI) of wild-type ERCC1 cDNA in the vector pET3C-ERCC1 which contains a unique *Nde*I site at the translation initiation site. This *Nde*I site and a *Cla*I site were used to isolate ERCC1His cDNA, recessive ends were filled in by Klenow fragment, and the cDNA was cloned into the blunt-ended *Bam*HI site of the donor plasmid pFastBacI (BAC-TO-BAC Baculovirus Expression System, Life Technologies, Inc.), resulting in pFastBacI-ERCC1His. To introduce a 6xHis-HA epitope encoding DNA sequence at the 3′ end of XPF cDNA, first a (blunt) in-frame *Nru*I site was introduced at the 3′ end of the XPF coding region by means of polymerase chain reaction using the antisense primer 5′-CGATCGATTCGGAAGCGCTGCCTCCCTTTTTCCCTTTTCCTTTTGAT-3′. Two primers (1, HIS-HA sense: 5′-CACCACCATCACCATCACGGAGGCAGCGCTTACCCATAGATGTTCCAGATTACGCTAGCTGAATCGATG-3′; and 2, HIS-HA antisense: 5′-GATCCATCGATTCAGCTAGCGTAATCTGGAACATCGTATGGGTAAGCGCTGCCTCCGTGATGGTGATGGTGGTG-3′) were annealed and cloned into the *Nru*I site, resulting in construct pBL-XPFHisHA. This construct was sequenced to exclude the presence of cloning and polymerase chain reaction mistakes. An *Nco*I (present on translation initiation site)-*Cla*I digest (both blunt-ended by Klenow fragment) released the XPF-HisHA cDNA, which was cloned into the *Bam*HI site (also made blunt by Klenow fragment) of the donor plasmid pFastBacI (Life Technologies, Inc.), resulting in construct pFastBacI-XPFHisHA. pFastBacI-ERCC1His and pFastBacI-XPFHisHA plasmids were transfected separately into competent DH10Bac cells to allow site-specific transposition with the Bacmid bMON14272. The recombinant Bacmids (rBac-ERCC1His and rBac-XPFHisHA) were isolated and transfected into Sf21 cells, which resulted in the production of recombinant viruses, designated virBac-ERCC1His and virBacXPFHisHA, respectively.

Baculovirus Infection and Extract Preparation from the Infected Cells—Virus amplification was performed as described (instruction manual BAC-TO-BAC system, Life Technologies, Inc.). For production of the proteins, seven 175-cm^2 dishes with monolayers of Sf21 cells were co-infected with virBac-ERCC1His and virBacXPFHisHA, at a multiplicity of infection of 5–10. Two days post-infection, cells were collected by low-speed centrifugation and washed twice with ice-cold phosphate-buffered saline. Cell pellets were fractionated as described before (26). Briefly, pellets were lysed in 8 times packed cell volume of NP-lysis buffer (25 mM Tris, pH 8, 1 mM EDTA, 10% glycerol, 1% Nonidet P-40, 1 mM EDTA, 1 mM phenylmethylsulfonyl fluoride, 1 μg/ml aprotinin, 1 μg/mg leupeptin, and 1 μg/ml antipain), incubated on ice for 30 min, and centrifuged at 800 × *g* for 10 min. The resulting supernatant (S1), containing most of the ERCC1-XPF complex, was used for further purification.

Purification of Recombinant ERCC1-XPF Complex—Prior to loading, NaCl concentration of S1 protein extracts was adjusted to 0.15 M. Protein extracts were applied to a phosphocellulose column (1 ml of beads per 7 mg of protein, Whatman P-11), equilibrated in buffer A (20 mM HEPES-KOH, pH 7.8, 2 mM $MgCl_2$, 10% glycerol, 1 mM phenylmethylsulfonyl fluoride, 5 mM β-mercaptoethanol, 0.02% Nonidet P-40) containing 0.15 M KCl. Bound proteins were eluted in buffer A containing 0.6 M KCl. After co-incubation of this fraction overnight at 4 °C with Ni^{2+}-NTA-agarose (Qiagen; 1 ml/5 mg of protein) in the presence of 1 mM imidazole, the protein-beads slurry was packed in a column, which was then washed with buffer A containing 20 mM imidazole (0.6 M KCl) and buffer A containing 40 mM imidazole (0.1 M KCl). ERCC1 and XPF were eluted in buffer A containing 200 mM imidazole and 0.1 mM KCl. Insulin (0.1 mg/ml) was added and this fraction was dialyzed twice for 1 h against buffer B (20 mM HEPES-KOH, pH 7.8, 10% glycerol, 2 mM dithiothreitol, 0.02% Nonidet P-40, 50 mM KCl, 1 mM EDTA, 2 mM $MgCl_2$). Typically, 50–100 μg (20 ng/μl) of purified complex was obtained from 15 mg of S1 protein extract.

To analyze complex formation between ERCC1 and XPF, 200 μl of the purified fraction was applied onto a 4.2-ml 15–35% glycerol gradient in buffer B. The gradients were centrifuged for 20 h at 300,000 × *g* and 160-μl fractions were collected.

In Vitro and in Vivo Repair Correction Assays—To test repair-correcting activity *in vitro*, 60 ng of purified ERCC1-XPF complex was added to Manley-type cell extracts derived from the indicated mutant cell lines; the protein mixture was incubated with an undamaged and a *N*-acetoxy-2-acetylaminofluorene-damaged plasmid in the presence of ^{32}P-labeled deoxynucleotides. Specific ^{32}P incorporation into the damaged plasmid was used as a measure for DNA repair synthesis (for details, see Wood *et al.*, Ref. 27). *In vivo* repair activity was determined by micro-injection of purified ERCC1-XPF into the cytoplasm of XPF homopolykaryons (XP126LO fibroblasts) or into the cytoplasm of mouse embryonal fibroblasts (MEFs) derived from ERCC1-deficient mice (28). Repair activity was analyzed after 4 h by UV-induced (15 J/m^2) incorporation of [^{3}H]thymidine and autoradiography as described (29). The number of grains above the nuclei is a measure of unscheduled DNA synthesis and reflects the cellular repair capacity.

Nuclease Assays—DNA oligonucleotides were purified by denaturing PAGE and 100–150 ng of DNA substrate was ^{32}P-labeled using polynucleotide kinase or Klenow fragment, followed by phenol extraction in 100 μl and Sepharose G-50 column centrifugation. To allow self-annealing, oligonucleotides were heated for 3 min at 95 °C and put on ice. Labeled substrates were kept at 4 °C. For the construction of flap substrates, one of the oligonucleotides was labeled, a 2-fold molar excess of the unlabeled complementary oligonucleotides was added, and the mixture was heated at 95 °C for 5 min, followed by stepwise cooling to allow annealing (30 min at 60 °C, 30 min at 37 °C, 30 min at 25 °C, and 30 min on ice).

Nuclease reactions (15 μl) were carried out in optimized nuclease buffer (50 mM Tris, pH 8.0, 0.2 mM $MnCl_2$, 0.1 mg/ml bovine serum albumin, and 0.5 mM β-mercaptoethanol), containing 100 fmol of substrate DNA and 100 fmol of recombinant ERCC1-XPF complex. Reactions were incubated for 90 min at 28 °C and either stopped by adding 15 μl of 90% formamide, heated at 95 °C, and loaded onto 10–20% denaturing polyacrylamide gels, or 5% glycerol was added and samples were immediately loaded onto 15–20% non-denaturing polacrylamide gels. Reaction products were visualized by autoradiography or PhosphorImager.

RESULTS

Characterization of Purified Recombinant ERCC1-XPF—To reconstitute recombinant ERCC1-XPF protein complex, Sf21 insect cells were co-infected with ERCC1- and XPF-containing baculovirus expression constructs. Both ERCC1 and XPF cDNAs encoded C-terminal affinity tags, a 6xHis-tag and a 6xHis-HA-epitope double-tag, respectively, to facilitate purification of proteins. Neither of these tags interfered with the

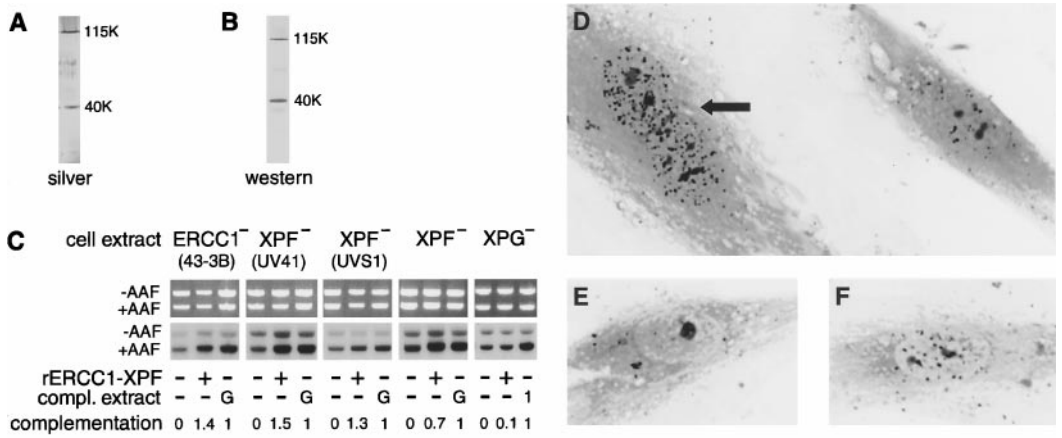

FIG. 1. **Characterization of purified recombinant ERCC1-XPF.** *A*, silver-stained protein profile of the top fraction from glycerol gradient. *B*, immunoblot analysis of same fraction, using anti-ERCC1 and anti-XPF antibodies. *C, in vitro* repair synthesis assay. *Upper panels* show ethidium bromide-stained DNA, *lower panels* show autoradiogram of same agarose gel. *43–3B*, Chinese hamster group 1 cell line; *UV41*, group 4 cell line; *UVS1*, group 4 cell line (former group 11); other cell lines originate from XP patients. *G* and *1* indicate that an XPG- and an ERCC1-deficient cell extract was used for complementation, respectively. Below each lane is indicated the amount of complementation obtained with purified ERCC1-XPF protein relative to that obtained with a complementing cell extract. *Numbers* were obtained by quantitation of specific incorporation of radiolabel into the *N*-acetoxy-2-acetylaminofluorene-damaged plasmid (*i.e.* incorporation in damaged minus undamaged plasmid), taking into account the amount of DNA present in each lane. Note that purified ERCC1-XPF complex is able to complement 43–3B and UVS1 cell extracts, as reflected by the increased levels of incorporation into damaged DNA. *D-F, in vivo* repair synthesis assay. *D*, XPF fibroblasts (*arrow* indicates injected multikaryon). *E*, uninjected; and *F*, injected ERCC1 MEFs. Nuclei were micro-injected with purified ERCC1-XPF. Number of grains *above* the nuclei, used as a measure for repair capacity, was increased 5–10 times both in XPF$^-$ primary fibroblasts and in ERCC1$^-$ MEFs upon injection of purified ERCC1-XPF.

function of the proteins *in vivo*, as micro-injection of XPF-(6xHis-HA) cDNA into the nucleus of XPF-deficient human fibroblasts and transfection of ERCC1-(6xHis) cDNA into ERCC1-deficient Chinese hamster cells fully corrected the repair defects of these mutant cell types (data not shown). A three-step purification protocol, which included phosphocellulose, nickel affinity chromatography, and a glycerol gradient, resulted in highly purified fractions containing 2 major proteins on silver stain with apparent molecular weight of approximately 40,000 and 115,000 (Fig. 1*A*). Immunoblot analysis with polyclonal antibodies confirmed these proteins to be ERCC1 and XPF (Fig. 1*B*). On the glycerol gradient the majority of ERCC1 and XPF was found to co-migrate, which demonstrated that the proteins reconstitute a stable ERCC1-XPF protein complex in insect cells. As only little further purification was obtained with this gradient and no significant differences were detected between the enzymatic activities of Ni-purified *versus* glycerol gradient-purified protein fractions, most experiments were performed with Ni-purified proteins. During the progress of this work also, recombinant ERCC1-XPF was purified from *Escherichia coli*, which was used to confirm that the activities described below were intrinsic to the ERCC1-XPF complex (data not shown).

The activity of recombinant ERCC1-XPF was tested in *in vitro* and *in vivo* repair assays. *In vitro*, ERCC1-XPF was found to correct the repair-deficient phenotype of cell extracts from human XP-F and Chinese hamster complementation groups 1 and 4, but not from XP-G (Fig. 1*C*). Correction was also found with an extract from the Chinese hamster mutant cell line UVS1, formerly known as the sole representative of complementation group 11, but recently shown to be functionally deficient in XPF as well (6). To test the activity of recombinant ERCC1-XPF *in vivo*, purified complex was micro-injected into primary fibroblasts derived from an XP-F patient. The injected cells showed a significant increase of unscheduled DNA synthesis after UV treatment, indicative for restored NER capacity (Fig. 1*D*). Chinese hamster cells are not very suitable for micro-injection for technical reasons, but the establishment of MEFs from a repair-deficient ERCC1$^-$ mouse (28) enabled us to analyze protein fractions for ERCC1-correcting activity *in vivo*. Micro-injection of purified ERCC1-XPF in these cells resulted in a significant increase in repair activity as well (Fig. 1*D*). These data demonstrate that the purified recombinant ERCC1-XPF complex effectively supports NER both *in vitro* and *in vivo*.

Recombinant ERCC1-XPF Incises DNA at Duplex Single Strand Junctions—Previously, we have shown that a His-tagged ERCC1-XPF complex purified from Chinese hamster ovary cells efficiently incises artificial DNA substrates containing a duplex single-stranded DNA junction (6). The observed ERCC1-XPF endonuclease activity was structure-specific and independent of other proteins like RPA. To test nuclease activity of our recombinant ERCC1-XPF, similar assays with such stem-loop substrates were performed. Rather than random DNA sequences, our artificial substrates exclusively contained thymine residues in the single-stranded regions to minimize formation of secondary DNA structures. Two major incisions were detected when recombinant ERCC1-XPF was applied to these substrates, being in one strand of the duplex region, two and three nucleotides (nt) away at the 5′ side of the junction (Fig. 2, *A* and *B*). This cleavage pattern was identical to that observed with endogenous ERCC1-XPF purified from Chinese hamster ovary cells (6).

To define optimal conditions for the nuclease activity we analyzed scissions at various concentrations of divalent metal ions. As also observed with the Chinese hamster ovary ERCC1-XPF complex, incision activity was absolutely dependent on the presence of divalent cations, as addition of EDTA completely blocked incisions (Fig. 2*C, lane 4*). Both Mg^{2+} and Mn^{2+} stimulated the endonuclease activity and, surprisingly, Mn^{2+} appeared to stimulate much better than Mg^{2+}. Optimal activity was observed in low concentrations of Mn^{2+} (0.2 mM) (Fig. 2*C, lane 14*) and was approximately 3 times higher than in the most optimal Mg^{2+} buffer (Fig. 2*C, lane 6*). In contrast, incision activity was inhibited by increasing amounts of Ca^{2+} (*lanes 9–12*), showing that Ca^{2+} cannot substitute for Mg^{2+} and Mn^{2+} in these reactions. The reaction products appearing at 0.2 mM Mn^{2+} were similar to those observed in all Mg^{2+} buffers tested (Fig. 2*C*), demonstrating that low Mn^{2+} concentrations were suitable for studying ERCC1-XPF activity. A control re-

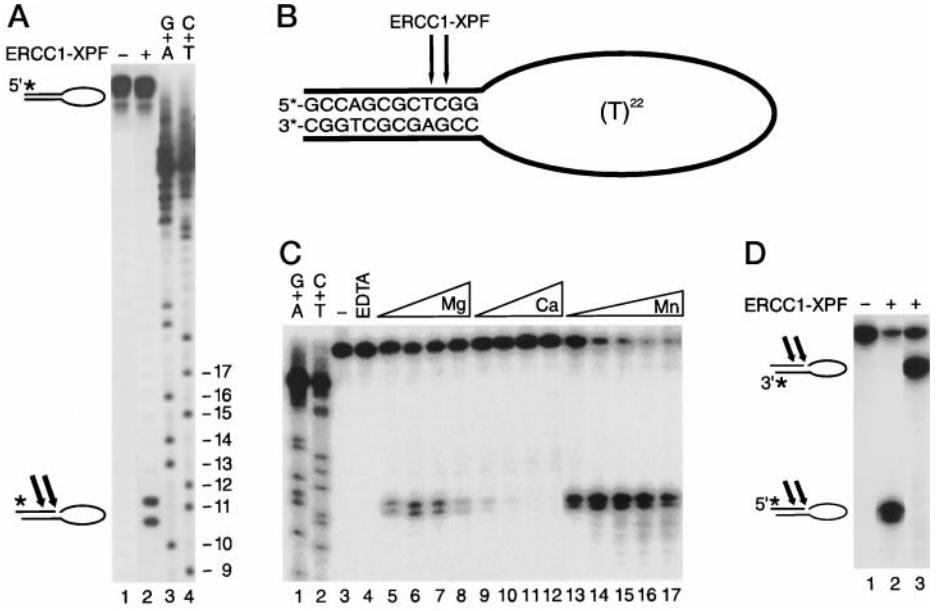

FIG. 2. **Recombinant ERCC1-XPF cleaves stem-loop substrate at DNA junction.** *A*, incision assay with stem 12-loop 22. *Lane 1*, no protein added. *Lane 2*, 20 ng of ERCC1-XPF. *Lanes 3* and *4*, Maxam-Gilbert sequence ladders, obtained from stem 21 to loop 4. Note that 5′-labeled Maxam-Gilbert sequence products run approximately 1.5 nt faster than ERCC1-XPF cleavage products. *Asterisks* indicate position of radioactive label in the substrate. *B*, schematic presentation of ERCC1-XPF incisions in stem 12-loop 22 substrate. *C*, divalent cation requirements for ERCC1-XPF cleavage. *Lanes 1–2*, Maxam-Gilbert ladders. *Lane 3*, no protein. *Lanes 4–17*, 20 ng of ERCC1-XPF. *Lane 4*, 5 mM EDTA. *Lanes 5–8*, 1, 2, 4, and 8 mM $MgCl_2$, respectively. *Lanes 9–12*, 1, 2, 4, and 8 mM $CaCl_2$. *Lanes 13–17*, 0.1, 0.2, 0.5, 1, and 2 mM $MnCl_2$. *D*, absence of aspecific (single-stranded) DNA degradation in 0.2 mM Mn^{2+}-nuclease buffer. *Lane 1*, 5′-labeled stem-loop substrate, no ERCC1-XPF. *Lane 2*, 5′-labeled stem-loop substrate with 20 ng of ERCC1-XPF. *Lane 3*, 3′-labeled stem-loop substrate with 20 ng of ERCC1-XPF.

action in 0.2 mM $MnCl_2$ without ERCC1-XPF (but with a corresponding amount of ERCC1-XPF dilution buffer B) showed that the DNA substrate is not subject to aspecific degradation under these conditions (Fig. 2*D, lane 1*); furthermore, when the same stem-loop substrate was labeled at the 3′ end, ERCC1-XPF cleavage at 0.2 mM Mn^{2+} resulted in a relatively large incision product consisting of the complete single-stranded loop and one strand of the stem, which demonstrated the absence of single-stranded endonucleolytic degradation (Fig. 2*D, lane 3*). In view of these results, all assays described below were performed in a standard buffer containing 0.2 mM $MnCl_2$.

Minimal Loop-size Incised by ERCC1-XPF—Determination of the minimal size of the single-stranded loop in a stem-loop substrate can provide indications about the minimal degree of helix opening required for ERCC1-XPF incision, a relevant parameter for NER. To investigate this, stem-loops with varying loop and stem sizes but with a similar DNA context around the junction were constructed (see Table I). If possible, the total amount of nucleotides was kept the same among these substrates. Incisions were observed on stems with a loop of 12, 18, 22, and 40 nucleotides, whereas a loop of 8 nucleotides only gave minor cleavage products (Fig. 3). All incisions were made at identical positions relative to the junction, 2 and 3 nucleotides away in the stem. Occasional incisions were seen in substrates with a loop size of 4 nucleotides (data not shown), but none were found in a 2-nucleotide loop and a fully paired hairpin structure (see also Fig. 4). This demonstrated that DNA substrates with less than 4–8 unpaired bases become poor DNA substrates for ERCC1-XPF mediated incision. Comparison of equally large stems (12 base pair) with different loop sizes (22 *versus* 40 nt) showed that incision efficiency increased with the size of the single-stranded loop (Fig. 3, *lanes 4* and *5*). We could not determine the minimal duplex size requirements for ERCC1-XPF activity as base pairing will be lost with very small stems, but apparently a 12-base pair stem is still sufficient for ERCC1-XPF mediated cleavage.

Minimal DNA Structural Elements Required for ERCC1-XPF-mediated Incision—A role for ERCC1-XPF has been anticipated not only in NER, but also in repair of interstrand cross-links and in single-strand annealing. The DNA intermediates that are recognized and cut by ERCC1-XPF during these events will probably differ from each other but they most likely share the simplest DNA structural motif that can be cleaved by the complex. Since the exact DNA structural elements required for endonucleolytic activity of ERCC1-XPF are still largely unknown, we decided to dissect the basic stem-loop substrate as listed in Fig. 4*A*.

A partially self-complementary oligonucleotide with two unpaired arms (splayed arm substrate) was incised by ERCC1-XPF only on one side of the duplex near the junction, causing removal of the 3′ protruding single-stranded arm. The polarity of this incision corresponded to those observed in stem-loop substrates. Comparison to Maxam-Gilbert ladders revealed that the major incision was made 4 nucleotides away from the DNA junction in the stem region (Fig. 4*B*). To investigate whether ERCC1-XPF required two or just one single-stranded arm for recognition and incision, self-annealing substrates were used having a constant duplex DNA region with either a 3′ or 5′ protruding single-stranded overhang (Fig. 4*A*). Consistent with the activity of Rad1-Rad10, ERCC1-XPF was found to remove the 3′ protruding single-stranded arm by incising this particular DNA strand in the duplex near the junction (Fig. 4*C*). Interestingly, incisions near the DNA junction were also detected in the substrate containing the 5′ protruding arm (Fig. 4*D*). In this case, cleavage did not result in removal, but rather extension of the single-stranded portion, as incisions were solely made in the opposite, non-protruding DNA strand. The polarity of cleavage was again consistent with the ERCC1-XPF-mediated incisions observed in stem-loops and splayed arms, being in one strand of duplex DNA at the 5′ side of a duplex single-stranded junction. Since we never observed incisions at blunt-ended duplex regions (for example, in the stem-loop substrates), we concluded that one single-stranded arm, moving away from the junction in either 3′ or 5′ direction, is necessary and sufficient for ERCC1-XPF to correctly position its nuclease activity on the DNA.

ERCC1-XPF Cleaves 3′-Flap Structures—To envisage its role in the single-strand annealing pathway, ERCC1-XPF has been proposed to remove 3′ protruding single-stranded arms from recombined duplex regions (13). To investigate whether ERCC1-XPF is able to cut these so-called flap structures, three (partially) complementary oligos were mixed and annealed (Fig. 5*A*). Analysis on native gels showed that this resulted in a mixture of all possible annealing products. Therefore both native and denaturing gels were used to analyze incisions (Fig. 5, *B* and *C*). In this way we found that ERCC1-XPF not only

TABLE I
Artificial DNA substrates

Nucleotides denoted in small letter type were filled-in by DNA polymerase I Klenow fragment, optionally with radioactive labeled dNTPs. Sizes of duplex regions are in base pairs, sizes of loops and overhangs in nucleotides. For the 3′-flap and 5′-flap, the oligonucleotide composition is given. Underlined sequences in F32 and F30 represent unpaired protruding arms.

stem21-loop4	5'-TCCTGGGTCGCCAGCGCTCGG$(T)_4$CCGAGCGCTGGCGACCCAGGa-3'	21 4
stem19-loop8	5'-TCGGGTCGCCAGCGCTCGG$(T)_8$CCGAGCGCTGGCGACCCGa-3'	19 8
stem17-loop12	5'-TGGTCGCCAGCGCTCGG$(T)_{12}$CCGAGCGCTGGCGACCa-3'	17 12
stem14-loop18	5'-TCGCCAGCGCTCGG$(T)_{18}$CCGAGCGCTGGCGa-3'	14 18
stem12-loop22	5'-GCCAGCGCTCGG$(T)_{22}$CCGAGCGCtggc-3'	12 22
stem12-loop40	5'-GCCAGCGCTCGG$(T)_{40}$CCGAGCGCtggc-3'	12 40
splayed-arm	5'-$(T)_{12}$GCCATCGCGAGTCC-GGACTCGCGATGGC$(T)_{12}$-3'	14 12 3' 12 5'
5'-overhang	5'-$(T)_{19}$GGCCGTGCTCTCCTGGATGTTCGAAAG-CTTTCGAACATCCAGGAGAGCACggcc-3'	27 3' 19 5'
3'-overhang	5'-GGCCGTGCTCTCCTGGATGTTCGAAAG-CTTTCGAACATCCAGGAGAGCACGGCC$(T)_{19}$-3'	27 19 3' 5'
F19	5'-GCGATGCGGATCCAAGTCT-3'	
F32	5'-GCGATGCGGATCCAAGTCTATTAGCGACAATG-3'	F32 F17 F36
F36	5'-CCTAGACTTAAGAGGCCAGACTTGGATCCGCATCGC-3'	
F17	5'-GGCCTCTTAAGTCTAGG-3'	
F30	5'-GTAACAGCGATTAGGCCTCTTAAGTCTAGG-3'	5' F19 F30 F36

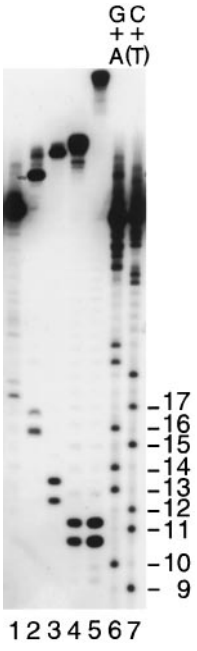

FIG. 3. **Determination of the minimal single-stranded loop size.** *Lanes 1–5*, 20 ng of ERCC1-XPF added. *Lane 1*, stem 19-loop 8. *Lane 2*, stem 17-loop 12. *Lane 3*, stem 14-loop 18. *Lane 4*, stem 12-loop 22. *Lane 5*, stem 12-loop 40.

incised the splayed arm substrates present in the mixture, but also the proposed intermediate in single strand annealing, the flap structure, thereby removing the 3′ protruding single-stranded arm from the duplex region. Major incisions in both this splayed arm and flap substrate were made 7 and 8 nucleotides away from the junction (Fig. 5*D*). The flap substrate was cleaved less efficiently than the splayed arm substrate (Fig. 5*B*), which shows that ERCC1-XPF prefers two single-stranded rather than two duplex arms at a DNA junction. No release of a single-stranded arm protruding 5′ from a flap substrate was observed, showing that also these substrates are recognized and cleaved with a defined polarity.

DISCUSSION

ERCC1-XPF Is a Structure-specific Endonuclease—Structure-specific DNA nucleases have been implicated in a variety of DNA metabolizing processes, including replication, recombination, and repair (30). Recently, we showed that ERCC1-XPF purified from Chinese hamster cells specifically incised DNA at duplex single-stranded borders, hence defining it as a structure-specific endonuclease (6). Others, however, reported that ERCC1-XPF cleaved single-stranded DNA (31) and that RPA confered structure-specific endonuclease activity to ERCC1-XPF (11). Here we demonstrate that a recombinant ERCC1-XPF complex, highly purified from insect cells, makes incisions specifically near DNA junctions in stem-loops, splayed arms, flaps, and single-stranded overhanging DNA substrates. Incisions were found in the absence of other proteins, showing that this activity is intrinsic to ERCC1-XPF. No scissions were observed in the single-stranded DNA regions of our substrates. We would like to propose two possible explanations for the fact that we find intrinsic structure-specific endonucleolytic activity with purified ERCC1-XPF, whereas others do not. First, by using stretches of thymines rather than random sequences we think we have minimized the formation of secondary structure in the single-stranded DNA portions of the substrates. Well defined single-stranded character was shown to be an important parameter for optimal activity of structure-specific nucleases (8). Second, to detect incisions, optimized buffer conditions appeared to be crucial. Hardly any incisions were detectable when reactions were performed in the presence of 10 mM Mg^{2+}, whereas clear activity was observed with low Mg^{2+} (1–2 mM) and especially with low Mn^{2+} (0.2–1 mM) concentrations. Thus, our data firmly establish ERCC1-XPF, like its yeast homolog Rad1-Rad10 (22), as a protein complex with intrinsic structure-specific endonuclease activity. Concerning replication protein A, we found that the effect of RPA on ERCC1-XPF activity was strongly dependent on the DNA substrate used. Although RPA was never found to be required for confering structure-specific endonuclease activity to ERCC1-XPF, we did observe a stimulatory effect on the nuclease activity, specifically in those cases where ERCC1-XPF cleavage occurred in the strand opposite the one RPA was bound to. Conversely, RPA blocked incision

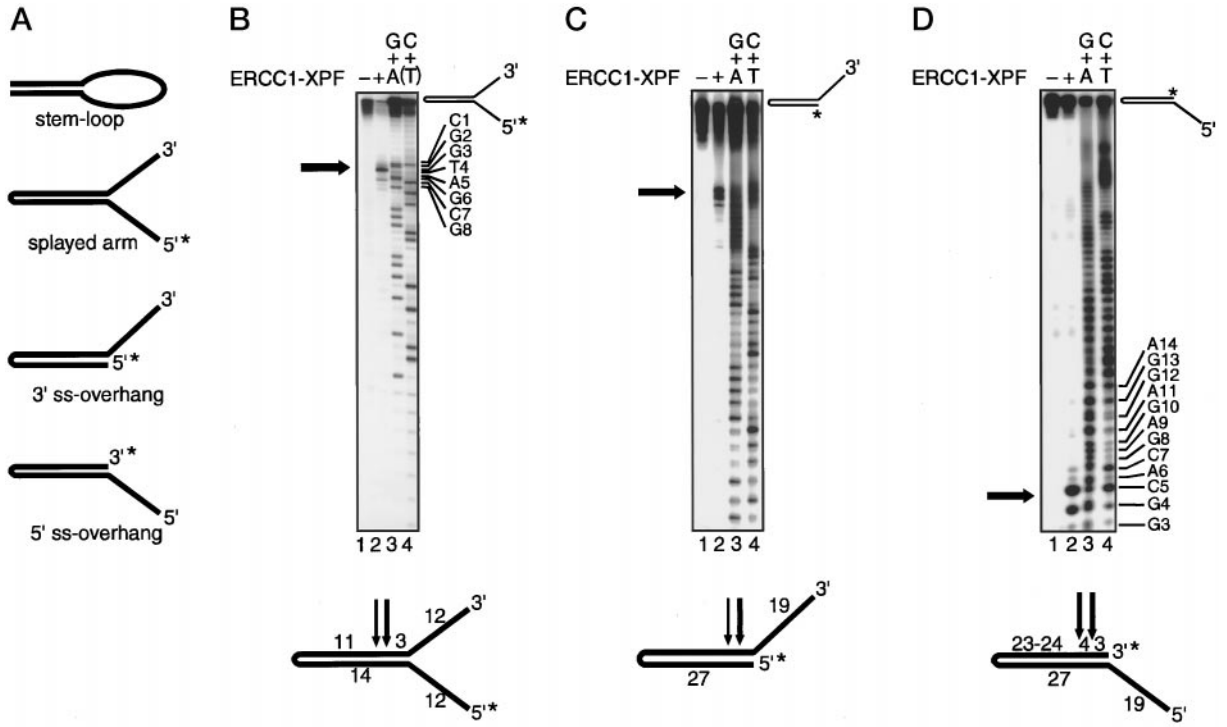

FIG. 4. **Minimal DNA structural elements required for ERCC1-XPF activity.** *A*, schematic presentation of "dissected" stem-loop substrate. *B*, splayed arm substrate, 5′ radiolabeled. *C*, 3′-overhang substrate, 5′ radiolabeled. *D*, 5′-overhang substrate, 3′ radiolabeled. For each panel (*B-D*): *lane 1*, no protein added. *Lane 2*, 20 ng of ERCC1-XPF. *Lanes 3* and *4*, Maxam-Gilbert ladders of corresponding substrate; counting starts at junction (note that in *C*, the 3′-overhang substrate, separation of Maxam-Gilbert ladders is insufficient to exactly determine cleavage positions).

activities that were directed to the same strand it was bound to. Details on this intricate cross-talk between RPA and ERCC1-XPF will be published elsewhere.

Comparison with Other Structure-specific Nucleases—An extensively studied family of structure-specific nucleases is the FEN-1 family. Its members, which include the repair proteins Rad2 in *S. cerevisiae* and mammalian XPG, share three large stretches of homologous amino acids with FEN-1 (20). Like ERCC1-XPF, these enzymes cleave branched DNA structures, but they do this at the opposite side of the junction, where the single-stranded DNA is moving away in a 3′ to 5′ direction (7, 19). Consistent with this cleavage polarity, XPG has been shown to make the 3′ incision during NER (7). Although FEN-1 and XPG act similarly on certain DNA structures (flaps, splayed arms), distinct activities on other DNA substrates hint at their different activities in the cell. For example, FEN-1 prefers flap substrates and does not cleave bubble substrates nor other substrates with a closed loop, which probably reflects the requirement of free single-stranded DNA ends for FEN-1 DNA-binding (19, 32). Also, no FEN-1 incisions were observed in substrates containing one single-stranded overhang, showing that FEN-1 only cleaves certain types of single-stranded duplex DNA junctions. A functional relevance for FEN-1-mediated incisions was recently provided with the finding that completion of a subpathway of DNA base excision repair *in vitro* requires FEN-1-dependent removal of splayed arm intermediates; XPG could not substitute for FEN-1 in this reaction (18).

As the engagement of ERCC1-XPF in recombinational events is still poorly understood, it is of particular importance to define the DNA substrate specificity of this protein complex. On the amino acid sequence level, ERCC1 shares a relatively small region of homology with FEN-1 and XPG, encompassing a helix-hairpin-helix motif. This motif, present twice in ERCC1, has been implicated in non-sequence-specific DNA binding (25). Functionally, the ERCC1-XPF complex is most

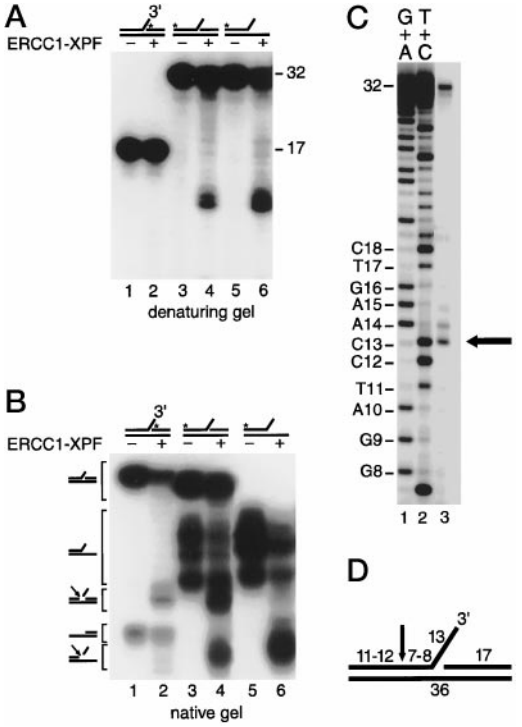

FIG. 5. **ERCC1-XPF cleaves 3′-flap substrates.** *A*, denaturing PAGE analysis of 3′-flap incisions. *B*, native PAGE analysis of 3′-flap incisions. For *A* and *B*: *lane 1*, 3′-flap, F17 radiolabeled, no protein. *Lane 2*, 3′-flap, F17 labeled, 20 ng of ERCC1-XPF. *Lane 3*, 3′-flap, F32-labeled, no protein. *Lane 4*, 3′-flap, F32 labeled, 20 ng of ERCC1-XPF. *Lane 5*, splayed arm, F32 labeled, no protein. *Lane 6*, splayed arm, F32 labeled, 20 ng of ERCC1-XPF. Note that especially splayed arm substrate shows a heterogeneous migration pattern on native PAGE (*B*, *lanes 3* and *5*). *C*, determination of exact cleavage positions. *Lanes 1* and *2*, Maxam-Gilbert ladders of F32. *Lane 3*, ERCC1-XPF cleavage pattern of 3′-flap, F32 radiolabeled. *D*, schematic presentation of ERCC1-XPF incisions in 3′-flap substrates.

readily compared with XPG. Like XPG, and perhaps expected from its involvement in NER, ERCC1-XPF efficiently cuts bubble substrates (6) and stem-loops, demonstrating that these NER nucleases do not require free single-stranded DNA ends for their activities. We found that ERCC1-XPF incises splayed arms and flaps, thereby cleaving off the 3′ protruding single-stranded arm in each case. ERCC1-XPF incisions were also observed in substrates with a 3′ or a 5′ overhanging arm only, resulting in removal or extension of the single-stranded portion, respectively. In contrast to FEN-1, we found that also XPG incised these substrates, and in agreement with its reported cleavage polarity, this caused extension of the 3′ arm and removal of the 5′ arm, respectively (data not shown). Apparently, contribution of DNA breathing in these cases is limited and the observed incision activities of ERCC1-XPF and XPG are specific for these overhanging substrates, as we could not detect comparable incisions at the blunt-ended duplex DNA of, for example, stem-loop substrates. Thus, a junction with one single-stranded arm, branching away from duplex DNA either in the 3′ or the 5′ direction, is necessary and sufficient for correct positioning of incisions by ERCC1-XPF and XPG. We postulate that in *S. cerevisiae*, the same will hold for Rad2 and Rad1-Rad10. The latter complex was previously shown to cut branched DNA substrates (22), but an activity on 5′ overhanging substrates has not been reported yet. Intriguingly, Rad10 lacks the helix-hairpin-helix motif that ERCC1 shares with other structure-specific nucleases. As the substrate specificities of ERCC1-XPF and Rad1-Rad10 appear to be similar, either this motif is not absolutely required for structure-specific nuclease activity, or alternatively, it is cryptically present elsewhere in the Rad1-Rad10 complex.

Incision Position Partially Depends on DNA Sequence—Running Maxam-Gilbert sequence ladders along our assays allowed a detailed analysis of the cleavage patterns. ERCC1-XPF-mediated incisions always occurred in the duplex some nucleotides away from the junction, varying from 2 to 3 nucleotides in stem-loop substrates, to 7–8 nucleotides in the case of the flap substrate. Given the fact that the DNA sequence around the junction was identical for the different stem-loop substrates, the observation that changing the structural properties by altering loop and stem sizes did not affect the cleavage pattern, may indicate that the site of cleavage is to some extent sequence-dependent. In support of this notion, the splayed arm and the flap substrates, composed of the same oligonucleotides, were also cleaved at identical positions (see Fig. 5). A splayed arm substrate with a different sequence composition around the junction was cleaved at 3 nt, rather than 7–8 nt, away from the junction (see Fig. 4). In all these cases, the major incisions were made at the 3′ side of a pyrimidine residue, suggesting that ERCC1-XPF prefers to cleave at cytosines and thymines. Two major incisions were observed with the 5′ overhanging substrate, one at a pyrimidine and the other at a purine residue. Whether the latter incision shows that the suggested pyrimidine preference is less strict in substrates with one single-stranded arm only or that this preference is based on coincidence, remains to be investigated.

ERCC1-XPF in Nucleotide Excision Repair—During NER, the two incisions around the lesion are made in a near synchronous manner. Several reports suggest that they occur in an ordered fashion, with most likely the 3′ (XPG-mediated) incision being made prior to the 5′ (ERCC1-XPF-mediated) incision (3, 33, 34). Depending on the type of lesion, XPG incisions have been found 2–9 nucleotides away from the lesion, whereas ERCC1-XPF cuts appear 15–24 nucleotides away on the opposite side of the lesion (3, 33, 35). The positions of these incisions correspond to the borders of the open DNA complex, which is formed during NER and spans approximately 25 nucleotides across the lesion (8). The question why such a relatively large region is unwound and excised is still unanswered, but one possibility could be that the size of the open complex reflects the minimal amount of unwinding required for XPG and ERCC1-XPF cutting activity. We found, however, that ERCC1-XPF incised substrates with loops as small as 4–8 nucleotides. Also XPG was previously shown to require only 5–10 unpaired nucleotides for efficient cleavage (8). Therefore, most likely other repair factors determine the actual size of the excised patch and they may do so by positioning the nucleases onto the borders of the unwound DNA intermediate. For ERCC1-XPF, two obvious candidates are the lesion-recognizing protein XPA and the single-stranded binding protein RPA, which both interact with this nuclease complex (9–12). The fact that the size of the patch (24–32 nt) strongly correlates to the length of the optimal single-stranded binding region of RPA (30 nt) (36) also suggests an important role of RPA in positioning the NER incisions.

ERCC1-XPF in Recombinational Pathways—ERCC1-XPF and its homologs have been implicated in such diverse processes as mating type switching in *Schizosaccharomyces pombe* (37) and DNA interstrand cross-link repair in mammals. It has been suggested that common recombinational mechanisms underly these processes. Direct evidence for a role of ERCC1-XPF in recombination comes from studies in *S. cerevisiae*, where it was shown that strains defective in Rad1 or Rad10 failed to complete recombination between direct DNA repeats, presumably due to their inability to remove nonhomologous DNA from the 3′ ends of recombined DNA intermediates (13). Here we tested directly whether ERCC1-XPF was able to remove protruding DNA sequences from duplex regions and found that the complex, like Rad1-Rad10, can indeed cut flap substrates with single-stranded arms protruding in the 3′ direction. The relevance of investigating the role of ERCC1-XPF in processes other than NER becomes most apparent from studies on ERCC1-deficient mice. On top of the classic NER-deficient phenotype observed with XPA-, as well as XPC-knock-out mice, characterized most profoundly by photosensitivity and predisposition to UV-induced skin cancer, ERCC1-deficient mice suffer from liver, spleen, and kidney abnormalities, developmental delay, reduced life span, and signs of premature senescence (28, 38). Accumulation of endogenously generated interstrand cross-links has been proposed to underly these non-NER-specific clinical manifestations (28). Whether flap structures are intermediates in, for example, interstrand cross-link repair remains to be shown, but the DNA substrate specificity described in this paper will allow a more direct search for the role of ERCC1-XPF in recombinational events.

Acknowledgments—We thank the members of our laboratory for advice and reagents: Suzanne Rademakers for performing the microinjection experiments, Eric Weterings for purifying ERCC1-XPF from *E. coli*, Anja Raams for preparation of cell extracts, Geert Weeda and Jan de Wit for providing ERCC1-deficient MEFs, Mirko Kuit for help with illustrations, and Dirk Bootsma for stimulating interest. We also thank Richard D. Wood and Maureen Biggerstaff (Imperial Cancer Research Fund, Clare Hall Laboratories, UK) for useful discussions and help with the initial part of this project.

REFERENCES

1. Friedberg, E. C., Walker G. C., and Siede, W. (1985) *DNA Repair and Mutagenesis*, ASM Press, Washington, D. C.
2. Huang, J. C., Svoboda, D. L., Reardon, J. T., and Sancar, A. (1992) *Proc. Natl. Acad. Sci. U. S. A.* **89,** 3664–3668
3. Moggs, J. G., Yarema, K. J., Essigmann, J. M., and Wood, R. D. (1996) *J. Biol. Chem.* **271,** 7177–7186
4. Aboussekhra, A., Biggerstaff, M., Shivji, M. K. K., Vilpo, J. A., Moncollin, V., Podust, V. N., Protic, M., Hubscher, U., Egly, J.-M., and Wood, R. D. (1995) *Cell* **80,** 859–868
5. Mu, D., Park, C.-H., Matsunaga, T., Hsu, D. S., Reardon, J. T., and Sancar, A. (1995) *J. Biol. Chem.* **270,** 2415–2418

6. Sijbers, A. M., De Laat, W. L., Ariza, R. R., Biggerstaff, M., Wei, Y.-F., Moggs, J. G., Carter, K. C., Shell, B. K., Evans, E., De Jong, M. C., Rademakers, S., De Rooij, J., Jaspers, N. G. J., Hoeijmakers, J. H. J., and Wood, R. D. (1996) *Cell* **86,** 811–822
7. O'Donovan, A., Davies, A. A., Moggs, J. G., West, S. C., and Wood, R. D. (1994) *Nature* **371,** 432–435
8. Evans, E., Fellows, J., Coffer, A., and Wood, R. D. (1997) *EMBO J.* **16,** 625–638
9. Li, L., Elledge, S. J., Peterson, C. A., Bales, E. S., and Legerski, R. J. (1994) *Proc. Natl. Acad. Sci. U. S. A.* **91,** 5012–5016
10. Park, C. H., and Sancar, A. (1994) *Proc. Natl. Acad. Sci. U. S. A.* **91,** 5017–5021
11. Matsunaga, T., Park, C.-H., Bessho, T., Mu, D., and Sancar, A. (1996) *J. Biol. Chem.* **271,** 11047–11050
12. Bessho, T., Sancar, A., Thompson, L. H., and Thelen, M. P. (1997) *J. Biol. Chem.* **272,** 3833–3837
13. Fishman-Lobell, J., and Haber, J. E. (1992) *Science* **258,** 480–484
14. Ivanov, E. L., and Haber, J. E. (1995) *Mol. Cell. Biol.* **15,** 2245–2251
15. Davies, A. A., Friedberg, E. C., Tomkinson, A. E., Wood, R. D., and West, S. C. (1995) *J. Biol. Chem.* **270,** 24638–24641
16. Busch, D., Greiner, C., Lewis, K., Ford, R., Adair, G., and Thompson, L. (1989) *Mutagenesis* **4,** 349–354
17. Ishimi, Y., Claude., A., Bullock, P., and Hurwitz, J. (1988) *J. Biol. Chem.* **263,** 19723–19733
18. Klungland, A., and Lindahl, T. (1997) *EMBO J.* **16,** 3341–3348
19. Harrington, J. J., and Lieber, M. R. (1994) *EMBO J.* **13,** 1235–1246
20. Harrington, J. J., and Lieber, M. R. (1994) *Genes Dev.* **8,** 1344–1355
21. Habraken, Y., Sung, P., Prakash, L., and Prakash, S. (1995) *J. Biol. Chem.* **270,** 30194–30198
22. Bardwell, A. J., Bardwell, L., Tomkinson, A. E., and Friedberg, E. C. (1994) *Science* **265,** 2082–2085
23. van Duin, M., van den Tol, J., Warmerdam, P., Odijk, H., Meijer, D., Westerveld, A., Bootsma, D., and Hoeijmakers, J. H. J. (1988) *Nucleic Acids Res.* **16,** 5305–5322
24. Sijbers, A. M., Van der Spek, P. J., Odijk, H., Van den Berg, J., Van Duin, M., Westerveld, A., Jaspers, N. G. J., Bootsma, D., and Hoeijmakers, J. H. J. (1996) *Nucleic Acids Res.* **24,** 3370–3380
25. Doherty, A., Serpell, L. C., and Ponting, C. P. (1996) *Nucleic Acids Res.* **24,** 2488–2497
26. Sugasawa, K., Masutani, C., Uchida, A., Maekawa, T., van der Spek, P. J., Bootsma, D., Hoeijmakers, J. H. J., and Hanaoka, F. (1996) *Mol. Cell. Biol.* **16,** 4852–4861
27. Wood, R. D., Biggerstaff, M., and Shivji, M. K. (1995) *Methods* **7,** 163–175
28. Weeda, G., Donker, I., de Wit, J., Morreau, H., Janssens, R., Vissers, C. J., Nigg, A., van Steeg, H., Bootsma, D., Hoeijmakers, J. H. J. (1997) *Curr. Biol.* **7,** 427–439
29. Vermeulen, W., Scott, R. J., Potger, S., Muller, H. J., Cole, J., Arlett, C. F., Kleijer, W. J., Bootsma, D., Hoeijmakers, J. H. J., and Weeda, G. (1994) *Am. J. Hum. Gen.* **54,** 191–200
30. Lieber, M. (1997) *Bioessays* **19,** 233–240
31. Park, C. H., Bessho, T., Matsunaga, T., and Sancar, A. (1995) *J. Biol. Chem.* **270,** 22657–22660
32. Murante, R. S., Rust, L., and Bambara, R. A. (1995) *J. Biol. Chem.* **270,** 30377–30383
33. Matsunaga, T., Mu, D., Park, C.-H., Reardon, J. T., and Sancar, A. (1995) *J. Biol. Chem.* **270,** 20862–20869
34. Mu, D., Hsu, D. S., and Sancar, A. (1996) *J. Biol. Chem.* **271,** 8285–8294
35. Svoboda, D. L., Taylor, J. S., Hearst, J. E., and Sancar, A. (1993) *J. Biol. Chem.* **268,** 1931–1936
36. Kim, C., Snyder, R. O., and Wold, M. S. (1992) *Mol. Cell. Biol.* **12,** 3050–3059
37. Gutz, H., and Schmidt, H. (1985) *Curr. Genet.* **9,** 325–331
38. McWhir, J., Seldridge, J., Harrison, D. J., Squires, S., and Melton, D. W. (1993) *Nat. Gen.* **5,** 217–223